Millennial-scale sea surface temperature and Patagonian Ice Sheet changes off southernmost Chile (53°S) over the past ~60 kyr

M. Caniupán,[1] F. Lamy,[1] C. B. Lange,[2] J. Kaiser,[3] H. Arz,[3] R. Kilian,[4] O. Baeza Urrea,[4] C. Aracena,[5] D. Hebbeln,[6] C. Kissel,[7] C. Laj,[7] G. Mollenhauer,[1] and R. Tiedemann[1]

Received 22 August 2010; revised 11 June 2011; accepted 20 June 2011; published 15 September 2011.

[1] Glacial millennial-scale paleoceanographic changes in the Southeast Pacific and the adjacent Southern Ocean are poorly known due to the scarcity of well-dated and high resolution sediment records. Here we present new surface water records from sediment core MD07-3128 recovered at 53°S off the Pacific entrance of the Strait of Magellan. The alkenone-derived sea surface temperature (SST) record reveals a very strong warming of ca. 8°C over the last Termination and substantial millennial-scale variability in the glacial section largely consistent with our planktonic foraminifera oxygen isotope (δ^{18}O) record of *Neogloboquadrina pachyderma* (sin.). The timing and structure of the Termination and some of the millennial-scale SST fluctuations are very similar to those observed in the well-dated SST record from ODP Site 1233 (41°S) and the temperature record from Drowning Maud Land Antarctic ice core supporting the hemispheric-wide Antarctic timing of SST changes. However, differences in our new SST record are also found including a long-term warming trend over Marine Isotope Stage (MIS) 3 followed by a cooling toward the Last Glacial Maximum (LGM). We suggest that these differences reflect regional cooling related to the proximal location of the southern Patagonian Ice Sheet and related meltwater supply at least during the LGM consistent with the fact that no longer SST cooling trend is observed in ODP Site 1233 or any SST Chilean record. This proximal ice sheet location is documented by generally higher contents of ice rafted debris (IRD) and tetra-unsaturated alkenones, and a slight trend toward lighter planktonic δ^{18}O during late MIS 3 and MIS 2.

Citation: Caniupán, M., et al. (2011), Millennial-scale sea surface temperature and Patagonian Ice Sheet changes off southernmost Chile (53°S) over the past ~60 kyr, *Paleoceanography*, *26*, PA3221, doi:10.1029/2010PA002049.

1. Introduction

[2] Past changes in surface ocean properties in the Southeast Pacific including the Southeast Pacific sector (SEPS) of the Southern Ocean (SO) just north of the modern Subantarctic Front are only poorly known primarily because high resolution sediment records from this region are very scarce [*Gersonde et al.*, 2005; *MARGO Project Members*, 2009]. In the SEPS, a few records have been retrieved around the Subantarctic Front (SAF) between ~100°W and ~120°W [*Gersonde et al.*, 2005; *Mashiotta et al.*, 1999]. Further north, high-resolution paleoceanographic records are available from the coastal ocean at the midlatitude Chilean margin between ~27°S and ~41°S [*Kaiser et al.*, 2005, 2008].

[3] The presently available SST data suggest a relatively weak LGM (19–23 kyr BP) cooling of generally less than ~2°C (based on diatoms transfer function SST; [*Gersonde et al.*, 2005]) and ~2.5°C (based on Mg/Ca SST; [*Mashiotta et al.*, 1999]) in the subantarctic SEPS. In contrast, alkenone-derived SST records from the midlatitude Chilean margin between ~30°S and ~41°S indicate substantially reduced LGM SSTs of the order of 4–6°C compared to modern values (5–7°C compared to early Holocene values) [*Kaiser et al.*, 2005, 2008; *Romero et al.*, 2006; *Mohtadi et al.*, 2008]. The large SST changes along the Chilean margin have been related to a ~5–6° northward shift of the northern margin of the Antarctic Circumpolar Current system (ACC) [e.g., *Lamy et al.*, 2004; *Kaiser et al.*, 2005]. It has been speculated that this northward extension of cold subantarctic water masses could be connected to an expansion of the sea ice cover around Antarctica and a northward displacement of the southern westerly winds (SWW). Such interpretation would be consistent with winter sea ice reconstructions in the Atlantic and Indian Ocean sectors of

[1]Alfred Wegener Institute for Polar and Marine Research, Bremerhaven, Germany.
[2]Department of Oceanography and Center for Oceanographic Research in the Eastern South Pacific, University of Concepción, Concepción, Chile.
[3]Leibniz Institute for Baltic Sea Research Warnemünde, Rostock-Warnemünde, Germany.
[4]Lehrstuhl für Geologie, Universität Trier, Trier, Germany.
[5]Graduate Programme in Oceanography, University of Concepción, Concepción, Chile.
[6]MARUM–Center for Marine Environmental Sciences, University of Bremen, Bremen, Germany.
[7]Laboratoire des Sciences du Climat et de l'Environnement, Institut Pierre Simon Laplace, Gif-sur-Yvette, France.

0883-8305/11/2010PA002049

the SO whereas the few records available suggest a more modest sea ice expansion in the Pacific sector during the LGM [*Gersonde et al.*, 2005].

[4] There is an ongoing debate on the pattern and timing of millennial-scale climate fluctuations in the Southern Hemisphere. In Antarctica, millennial-scale temperature changes over the last glacial have been consistently explained by the bipolar seesaw concept that suggests an out-of-phase millennial-scale climate pattern between the Northern and Southern hemispheres [e.g., *Stocker and Johnsen*, 2003; *EPICA Community Members*, 2006]. This Antarctic millennial-scale pattern seems to extend into the Southern Hemisphere midlatitudes (40°–46°S) as indicated by high-resolution SST records from the Chilean margin (ODP Site 1233; [*Lamy et al.*, 2004; *Kaiser et al.*, 2005]); New Zealand [*Pahnke et al.*, 2003] and the SW Indian Ocean [*Barrows et al.*, 2007a]. Millennial-scale SST amplitudes in these records are of the order of 2–3°C and are similar to Antarctic temperature changes at these time-scales [*Jouzel et al.*, 2007]. In the SO south of the SAF, however, high-resolution SST records with sufficient age control for analyzing the timing of millennial-scale pattern are still missing.

[5] In contrast to the findings of Antarctic millennial-scale pattern in SST records, continental glaciological and palynological data from the Chilean Lake District (~40°S; directly onshore of ODP Site 1233) have been used in support for inter-hemispheric synchrony both during the last glacial [*Lowell et al.*, 1995] and the deglaciation (e.g., cooling during the Younger Dryas (YD) cold phase; [*Denton et al.*, 1999; *Moreno et al.*, 2001]). However, new glaciological data from the southern Patagonian Ice Sheet (PIS, south of ~50°S) suggest glacier advances more in phase with Antarctic climate pattern [*Kaplan et al.*, 2008; *Moreno et al.*, 2009; *Sugden et al.*, 2009] and consistent with data from New Zealand [*Barrows et al.*, 2007b; *Kaplan et al.*, 2010].

[6] During the last glacial, the icefields in Patagonia expanded to form the larger Patagonian Ice Sheet (PIS) covering the southern Andes between ~38°S and ~56°S [e.g., *Glasser and Jansson*, 2008]. For the Atlantic side of the Andes, an updated view of glacial and deglacial changes in the extension of the southern PIS has been recently presented by *Sugden et al.* [2009] based on extensive dating of terrestrial records. This reconstruction suggests five major advances of the southern PIS during the last glacial and/or stagnation phases of ice retreat during the last deglacial. Glacial advances of the southern PIS have been linked to dust content changes as recorded in Antarctic ice cores [e.g., *Fischer et al.*, 2007], as glacier advances into the eastern Andean foreland largely enhance the availability of fine-grained material in the assumed Patagonian dust source areas [*Sugden et al.*, 2009; *Kaiser and Lamy*, 2010]. In contrast to the eastern side of the Andes, little is known about the extent of the PIS on the Pacific continental margin or the effect of its advances and retreats on the coast of the Chilean margin. Furthermore, IRD-based records of PIS changes on the Pacific side of the ice sheet are still missing.

[7] Here we present new surface water records including alkenone-based SST, planktonic foraminifera oxygen isotope and IRD records from the southernmost continental Chilean margin based on core MD07-3128 retrieved from the Pacific entrance of the Strait of Magellan (53°S) covering the past ~60 kyr. We discuss millennial-scale and longer term SST pattern and compare them to the well-dated SST record from ODP Site 1233 at 41°S and to temperature changes in Antarctic ice core. We show that glacial SSTs were partly influenced by the presence of the large PIS located close to the site, at least during the LGM.

2. Study Area

[8] Modern surface circulation in the Southeast Pacific off southernmost Chile (~53°S) is dominated by the Cape Horn Current (CHC) a coastal branch of the Antarctic Circumpolar Current (ACC) [*Strub et al.*, 1998; *Antezana*, 1999; *Chaigneau and Pizarro*, 2005] (Figure 1a). The CHC originates from the bifurcation of the northern ACC approaching South America between 40° to 45°S. The northern branch forms the Peru-Chile (or Humboldt) Current flowing equatorward whereas the CHC flows poleward along the southernmost Chilean continental margin toward the Drake Passage and transports Subantarctic Surface water (SAAW) [*Shaffer et al.*, 1995; *Strub et al.*, 1998]. The area off the Strait of Magellan is located ~5° latitude north of the present SAF [*Orsi et al.*, 1995]. Modern mean annual SST in this area is ~8°C and the seasonal range is ~3°C (World Ocean Atlas 2009).

[9] Within the southern Chilean fjord region, the relatively saltier Pacific surface waters progressively mix with fresher waters from melting glaciers, precipitation, and river runoff to produce a positive estuarine circulation characterized by strong density, temperature and salinity gradients [*Pickard*, 1971; *Silva and Calvete*, 2002; *Sievers and Silva*, 2008]. However, the exchange between fjord waters and open Pacific water masses is quite restricted due to very shallow sill depths on the continental shelf off southernmost Chile (30–40 m [*Antezana*, 1999]). Slightly reduced salinities originating from the outflow of fjord waters occur along the continental margin (Figure 1b) and are restricted to a thin surface layer of up to ~50 m thickness [*Antezana*, 1999; *Kilian et al.*, 2007].

[10] At present, Patagonia has three main glacier systems: the Northern and Southern icefields (46°–52°S) and the Darwin Mountain ice field in Tierra del Fuego (54–55°S) that greatly expanded during the last glacial and formed the much larger PIS covering the entire Andean part of southern South America between ~38°S and 56°S [e.g., *Glasser and Jansson*, 2008] (Figure 1b). Though little is known about the extent of this ice sheet on the Pacific continental margin, it is assumed that glaciers advanced toward the continental shelf edge and terminated in iceberg-calving fronts [*DaSilva et al.*, 1997]. This would bring the ice sheet very proximal to our coring site and we thus expect a much larger meltwater influence on surface water salinities and possibly also on SSTs in the study area.

3. Material and Methods

[11] The 30.33m-long Calypso piston core MD07-3128 was retrieved in 2007 from the continental slope off the Strait of Magellan, southern South America, at 52°39.57′S, 075° 33.97′W (1,032 m water depth) during the IMAGES (International Marine Past Global Changes Studies) XV-MD159-Pachiderme cruise on board R/V *Marion Dufresne*.

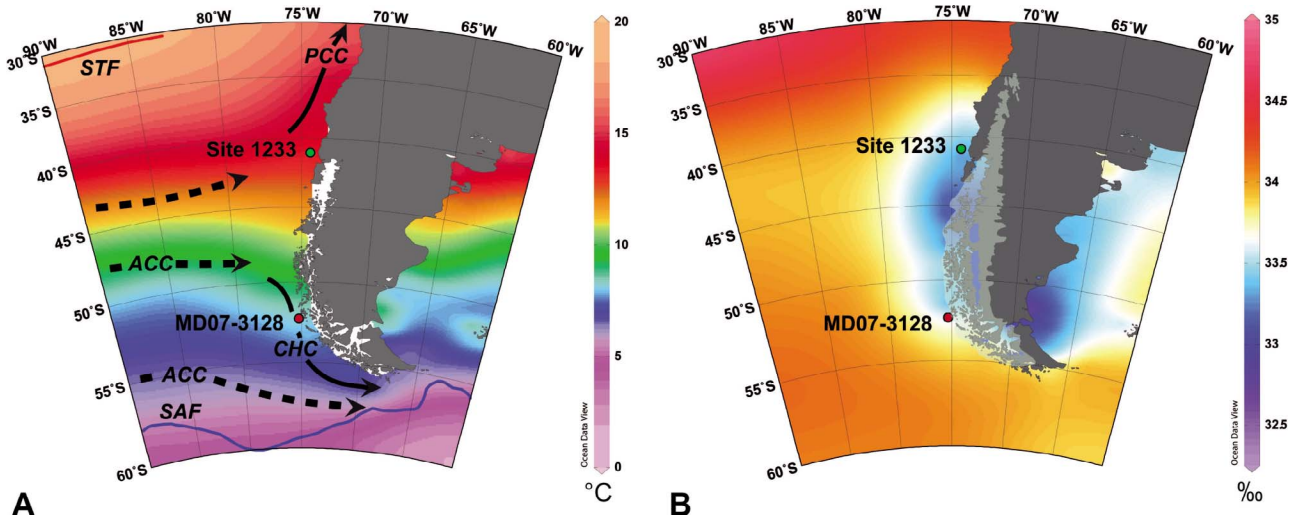

Figure 1. Core location maps. (a) Schematic illustration of the modern surface circulation in the Southeast Pacific after *Strub et al.* [1998] with mean annual SST (World Ocean Atlas 2009); PCC: Peru–Chile Current, ACC: Antarctic Circumpolar Current, CHC: Cape Horn Current. Location of major Southern Ocean fronts after *Orsi et al.* [1995]; STF = Subtropical Front (red), SAF = Subantarctic Front (blue). (b) Annual sea surface salinity (color bar) off southern South America (World Ocean Atlas 2009). Extension of the modern ice fields in Patagonia and maximum extent of the PIS during the LGM (based on *Hollin and Schilling* [1981] and *McCulloch et al.* [2000]) is shown in dark gray and light blue, respectively.

[12] The top 50 cm of the core (Holocene sediments) consist of olive yellow foraminifera ooze with >40% $CaCO_3$ content. The rest of the sequence is mainly composed of silt-bearing clay with m-scale variations in color between gray and grayish olive. Drop-stones were visually observed in particular in the upper 10 m of the core (except for the Holocene foraminifera ooze interval) and to a lesser amount deeper in the core.

[13] For this study, core MD07-3128 was sub-sampled every 12 cm resulting in an average temporal resolution of ~2.8 kyr for the intervals corresponding to the Holocene, ~200 years for the period covering Marine Isotope Stage (MIS) 2, and ~230 years for the interval comprising MIS 3 (the oxygen isotope records are of lower resolution during this interval). All samples were stored frozen until chemical analysis.

3.1. Chronology

[14] The age control of the upper core section of core MD07-3128 (0.3 to 18.51 m) was based on 13 accelerator mass spectrometry (AMS) ^{14}C dates performed on mixed planktonic foraminifera (Table 1). Below ~18.5 m-core-depth, the radiometric chronology was supplemented by the record of the Laschamp magnetic field excursion located between 19.65 m (top) and 21.5 m (base). We define the Laschamp excursion as the directional maximum shift centered at 41.25 kyr [*Laj et al.*, 2000, 2009] and use the mid-point at ~20.6 m core depth as an age control point. Below the Laschamp excursion, we extended the age-scale to the base of the core by tuning our alkenone SST record to that of ODP Site 1233 on its latest age model [*Kaiser and Lamy*, 2010] (Figure 2a) using a minimum of only two correlation points (Table 1). This age model is consistent with the low resolution planktonic $\delta^{18}O$ record from our core

Table 1. Age Control Points of Core MD07-3128

Laboratory ID	Core Depth (m)	^{14}C AMS Age (kyr B.P.)	± Error (years)	Calibrated Age 1σ Range (cal. kyr B.P.)	Calibrated Age Average (cal. kyr B.P.)	Dating Method
KIA 34252	0.03	3.405	25	2.91–3.06	2.99	^{14}C AMS
KIA 36388	0.3	9.490	45	10.02–10.19	10.11	^{14}C AMS
KIA 34253	0.35	9.945	45	10.52–10.64	10.58	^{14}C AMS
KIA 36390	0.94	13.040	60	14.17–14.67	14.42	^{14}C AMS
KIA 34255	1.55	15.460	70	17.89–18.08	17.99	^{14}C AMS
KIA 36391	2.5	16.100	70	18.61–18.77	18.69	^{14}C AMS
KIA 34256	3.93	17.330	130	19.78–20.07	19.93	^{14}C AMS
KIA 36392	7	19.560	100	22.31–22.66	22.48	^{14}C AMS
KIA 36393	9.52	22.760	150	26.25–26.81	26.53	^{14}C AMS
KIA 36394	13.96	23.610	150	27.62–28.09	27.86	^{14}C AMS
KIA 39462	16.01	26.400	240	30.37–30.83	30.6	^{14}C AMS
KIA 36395	17.96	31.540	465	34.94–35.61	35.28	^{14}C AMS
KIA 39463	18.51	33.660	540	37.07–38.45	37.76	^{14}C AMS
	20.58				41.25	Paleomagnetic age (Laschamp excursion)
	27.0				49.93	SST tuning to ODP Site 1233
	30.12				59.66	SST tuning to ODP Site 1233

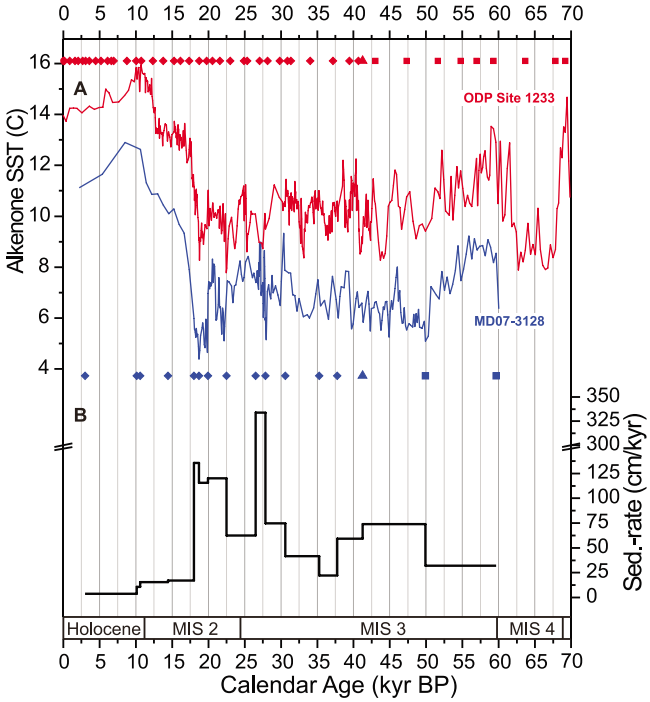

Figure 2. Age model for core MD07-3128. (a) Well-dated alkenone SST record of ODP Site 1233 (red curve [*Kaiser and Lamy*, 2010]) compared to our SST record of MD07-3128 (blue curve). Diamonds represent radiocarbon dates, triangles the location of the Laschamp paleomagnetic excursion, and squares tuning points. (b) Sedimentation-rates of core MD07-3128.

(Figure 3). All ^{14}C ages were converted to calendar ages using the Calib 6.02 software and the marine calibration data set MARINE09 [*Reimer et al.*, 2009] with a local marine reservoir deviation of 221 ± 40 years [*Ingram and Southon*, 1996]. We are aware that pre-Holocene and deglaciation reservoir ages might have been larger at our site. However, to the best of our knowledge, there is presently no information on regional changes in reservoir ages in the study area available. *De Pol-Holz et al.* [2010] suggest that large reservoir age changes in the order of >1000 years did probably not occur at the Chilean margin at ~36°S. We therefore believe that our present age model is sufficient for the purpose of discussing glacial/interglacial and millennial-scale changes. Further work on Chilean continental margin records including site MD07-3128 will be required in the future in order to better constrain past reservoir age changes and their implications for intermediate and deep water circulation.

3.2. Alkenone-Sea Surface Temperatures (SSTs)

[15] We determined SST by alkenone paleothermometry in continuous 12 cm intervals. Long-chain alkenones were extracted from 3 to 5 g of pulverized freeze-dried sediments following published methods [*Müller et al.*, 1998].

[16] The relative abundances and concentrations (in ng/g dry sediment weight) of di-, tri-, and tetra-unsaturated C_{37} alkenones were measured using gas chromatography equipped with a fused silica capillary column (60 m × 0.32 mm, DB-5 MS, Agilent J&W) and flame ionization detection (FID). 2-nanodecanone added to the samples before extraction was used as internal standard. Helium was employed as carrier gas with a constant pressure of 150 kPa. After injection at 50°C, the oven temperature was programmed to 250°C at a rate of 25°C/min to 290°C at a rate of 1°C/min, held for 26 min, and finally to 310 at a rate of 30°C/min, where the final temperature was maintained for 10 min.

[17] The $U^{K'}_{37}$ index, based on the concentration of di- and tri-unsaturated ketones with 37 carbon atoms produced by some Haptophyte algae was used to estimate SST ($U^{K'}_{37}$ = $[C_{37:2}]/[C_{37:2} + C_{37:3}]$) [*Prahl and Wakeham*, 1987]. To translate $U^{K'}_{37}$ values to an estimation of SST we applied the calibration of *Prahl et al.* [1988] (SST = $(U^{K'}_{37}–0.039)/(0.034)$) that has been widely used for paleotemperature estimations. The reproducibility of the procedure was evaluated using a homogeneous sediment standard extracted every batch of 5 samples. The relatively analytical error was below 1°C.

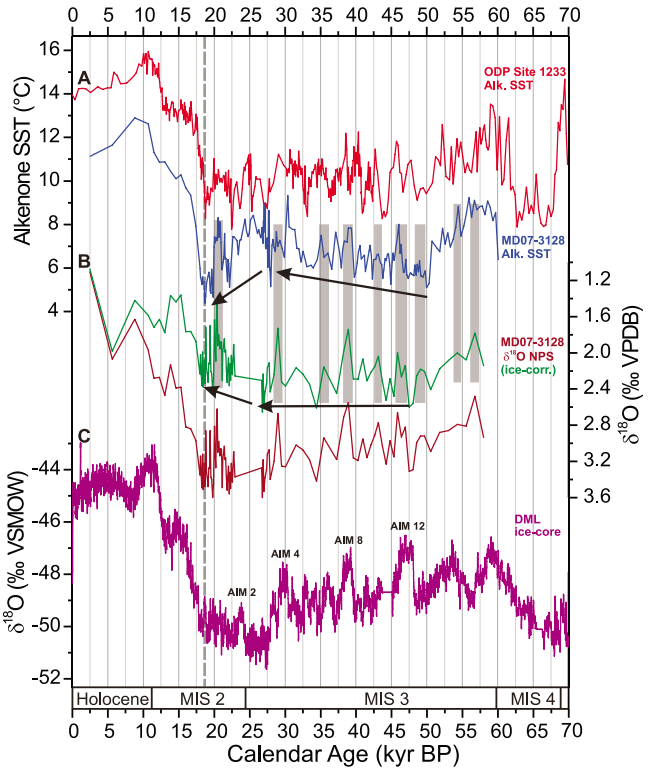

Figure 3. Comparison of SST proxy data from the Southeast Pacific to Antarctic ice core data for the past 70 kyr BP. (a) Alkenone-SST record from ODP Site 1233 located at 41°S [*Kaiser and Lamy*, 2010] and core MD07-3128 (53°S; this study). Black arrows mark the long-term warming trend observed over MIS 3 followed by a cooling trend to the LGM in our record. (b) $\delta^{18}O$ record of *Neogloboquadrina pachyderma* sinistral from core MD07-3128 (brown curve shows uncorrected data; green curve is ice-corrected). Black arrows mark long-term trends. Gray bars between A and B visualize common millennial-scale variability in the alkenone SST and the ice-corrected $\delta^{18}O$ record. (c) $\delta^{18}O$ record from the EPICA Dronning Maud Land (DML) ice core [*EPICA Community Members*, 2006] on the new Lemieux-Dundon time-scale [*Lemieux-Dudon et al.*, 2010]. Vertical dashed line refers to the beginning of the deglacial warming.

[18] We used $U^{K'}_{37}$ in preference to the original index because U^{K}_{37} includes the tetra-unsaturated C_{37} alkenone ($C_{37:4}$) that, although present in high abundances in cold regions [*Rosell-Melé*, 1998], is affected by other parameters in addition to temperature such as salinity [*Sikes et al.*, 1997; *Bendle et al.*, 2005; *McClymont et al.*, 2008]. The relative abundances of $C_{37:4}$ alkenone were compared to IRD estimates in order to constrain their applicability as a paleosalinity proxy.

3.3. Oxygen Isotopes

[19] Oxygen stable isotope ($\delta^{18}O$) analyses were performed at the University of Bergen on specimens of the planktonic foraminifera *Neogloboquadrina pachyderma* sinistral (*N. pachyderma* (sin.) selected from the >150–250 μm size fraction. Samples were analyzed using a Finnigan MAT 253 mass spectrometer coupled to an automated Kiel device. The data are reported on the VPDB scale calibrated with NBS-19. The long-term analytical precision of the system as defined by the reproducibility of carbonate standards between 6 and 60 mg is ±0.08‰ for $\delta^{18}O$.

[20] In order to derive the temperature and salinity related signal in the $\delta^{18}O$ record of *N. pachyderma* (sin.), we performed an ice-volume correction based on the global Holocene and deglacial sea level record of *Fairbanks* [1989] (0–22 kyr BP) and the global sea level record from the Red Sea [*Arz et al.*, 2007] for the earlier part of the record. We assume 1.2‰ ice-effect for the last termination.

[21] Furthermore, in order to compare potential paleosalinity changes at site MD07-3128 to the PIS meltwater record at ODP Site 1233 [*Lamy et al.*, 2004], we calculated $\delta^{18}O$ of seawater ($\delta^{18}O_{sw}$) for the late glacial back to ~25 kyr BP. For this purpose, stable oxygen isotope ($\delta^{18}O_{carb}$; ‰VPDB, converted to VSMOW by adding 0.27‰; [*Coplen et al.*, 1983] and alkenone-based sea surface temperature (T; °C) records have been interpolated and combined to reconstruct the $\delta^{18}O_{sw}$ (‰VSMOW) following the *Shackleton* [1974] equation:

$$T = 16.9 - 4.38^{*}\left(\delta^{18}O_{carb} - \delta^{18}O_{sw}\right) + 0.1^{*}\left(\delta^{18}O_{carb} - \delta^{18}O_{sw}\right)^{2}.$$

In order to eliminate the global ice volume signal from the $\delta^{18}O_{carb}$ record, the data were corrected assuming an enrichment of 0.1‰ per 10 m of sea level lowering. Again, the sea level reconstructions by *Fairbanks* [1989] (0–22 kyr BP) and the global sea level record from the Red Sea [*Arz et al.*, 2007] were used between 8 and 22 kyr and 22–25 kyr, respectively. The reconstructed $\delta^{18}O_{sw}$ is directly related to sea surface salinity changes [e.g., *Rostek et al.*, 1993]. A calibration for the local $\delta^{18}O_{sw}$ – salinity relationship is unfortunately not available.

3.4. Ice Rafted Debris

[22] We use the relative percentage of the >150 μm carbonate-free fraction and manual particle counts as proxies for ice rafted debris (IRD). The >150 μm was separated by wet-sieving after removal of carbonate with 10% acetic acid and organic matter with 3.5% hydrogen peroxide. IRD was counted from the >150 μm carbonate-free fraction, assuming that coarser-grained terrigenous sediment can only reach the core location through iceberg transport. Volcanic particles are not a significant component at Site MD07-3128 most likely because ash plumes originating from volcanoes of the Southern Andes are typically transported and deposited eastward due to the prevailing strong westerly winds [e.g., *Kilian et al.*, 2003]. Opal has not been resolved, but the opal contents are far too low to significantly contribute to the >150 μm carbonate-free fraction record. This assumption is confirmed by microscopic inspection of a number of selected samples.

4. Results

4.1. Chronology

[23] According to our age model, core MD07-3128 records the last ~60 kyr BP covering most of the last glacial (MIS 3 to MIS 2) to the late Holocene (Table 1 and Figure 2). Variable sedimentation rates along the core were recorded (Figure 2b), reaching mean values of ~60 cm kyr^{-1} during almost all MIS 3 with exceptionally high values of >330 cm/kyr between ~28 and ~27 kyr BP. Mean sedimentation rates were ~120 cm/kyr around the LGM decreasing to ~18 cm/kyr during the last termination, and to ~4 cm/kyr during the Holocene. The high mean sedimentation rates during the glacial period can be explained by the proximal location of our site to the PIS and accordingly strong terrigenous supply which is presently primarily trapped within the fjords [*Kilian et al.*, 2003, 2007]. The peak sedimentation rates between ~28 and ~27 kyr BP may further be related to relatively large one sigma ranges of the calibrated ages of the two radiocarbon datings and/or variable reservoir ages.

4.2. Alkenone SST and Planktonic Foraminiferal $\delta^{18}O$

[24] We reconstructed a continuous alkenone-derived SSTs record for the past ~60 kyr BP (Figure 3a). The SSTs oscillated between a minimum of 4.4°C at 18.8 kyr B.P and a maximum of 13°C at 9.6 kyr BP. The record exhibits an overall pattern of low temperatures, on average close to 7°C during the glacial period from ~60 kyr BP to ~19 kyr BP. Relatively warm temperatures (up to ~9°C) occur during early MIS 3 followed by a minimum of ~5°C close to 50 kyr BP. Thereafter, a long-term warming trend of ~2°C persists until ~25 kyr BP which is followed by a cooling trend of the order of ~3°C leading to the LGM with minimum SSTs around ~19 kyr BP. From 50 kyr BP to 19 kyr BP, pronounced millennial-scale variability is observed. The amplitudes of these short-term variations are mostly ~2–3°C with a few larger amplitude oscillations of about 4°C in the younger half of this period.

[25] After the coldest temperatures at ~19 kyr BP, a drastic increase in the SST of ca. 8°C is observed; this marks the beginning of Termination 1. Two warming steps characterized the deglacial period at 53°S: the first one displayed an increase of 4°C and lasted ca. 3 kyr and occurred between ~18.6 and ~15.3 kyr BP. The second step, with a duration of ca. 1.5 kyr, started at about 12.2 kyr BP and had an amplitude of ~2°C (Figure 3a). Finally, after a brief warm period most likely representing the Holocene Climate Optimum as observed in many records of the Southern Hemisphere [e.g., *Bianchi and Gersonde*, 2004; *Kaiser et al.*, 2005], alkenone-derived SSTs progressively declined toward cooler temperatures, reaching values close to 11°C in the late Holocene.

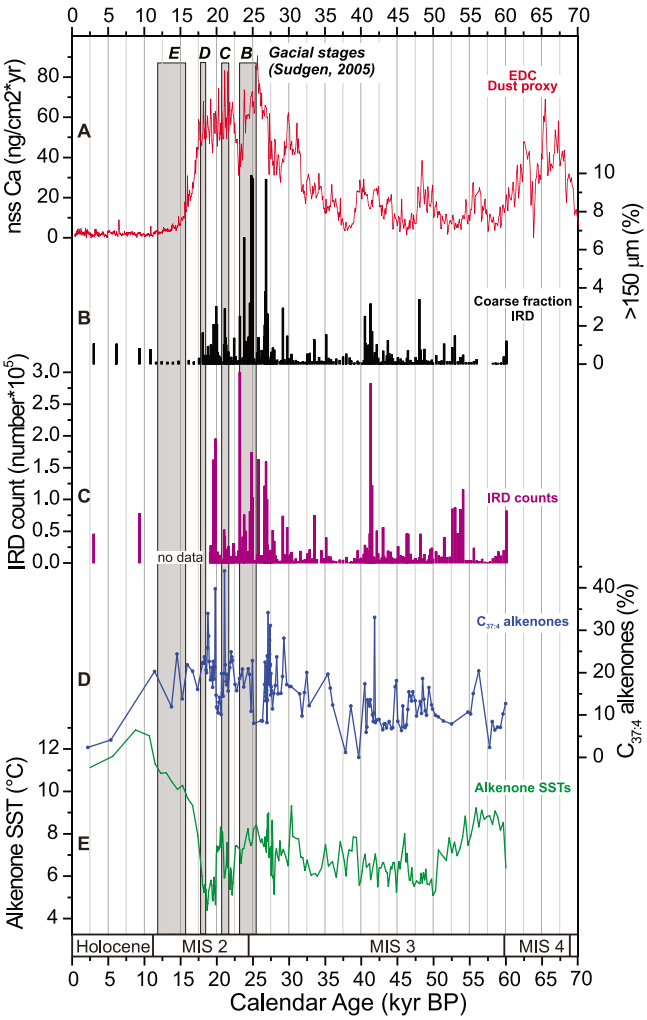

Figure 4. Proxies related to the dynamics of the PIS as recorded in core MD07-3128 compared to an Antarctic dust proxy record. (a) Non-sea-salt calcium from EPICA Dome C (EDC) (a proxy for dust content changes in Antarctic ice cores) [*Fischer et al.*, 2007]. (b) Percentage of >150 μm carbonate-free sediment fraction. (c) IRD counts. (d) Percentage of tetra-unsaturated C_{37} alkenones to total alkenones as a proxy for low-salinity water. (e) Alkenone-derived SST record from our site MD07-3128. Gray bars mark glacial stages as reconstructed from terrestrial records in Southern Patagonia [*Sugden et al.*, 2009].

[26] We compare our alkenone-based SST data to the ice-volume corrected planktonic δ^{18}O record of *N. pachyderma* (sin.) (Figure 3b). Although the resolution of the δ^{18}O record is lower than that of the alkenone SSTs (during MIS 3 and early MIS 2), both records share common millennial-scale variations. These short-term variations in the *N. pachyderma* (sin.) δ^{18}O record have amplitudes between ~0.4 and ~0.7‰. At Termination 1, δ^{18}O values rise by ~1‰ between ~18.3 and ~15.3 kyr BP, an interval in which alkenone SSTs increase by ~4°C. Thereafter, the record has very low resolution. Higher δ^{18}O values occur at ~12 kyr BP (three data points) and at ~5.6 kyr BP (only one data point). There is a slight long-term trend toward lower δ^{18}O values from late MIS 3 toward the LGM.

4.3. Ice Rafted Debris and Paleosalinity

[27] The IRD count record largely parallels the relative percentages of the >150 μm carbonate-free fraction (Figure 4). Most IRD consists of sand-sized particles with generally minor amounts of gravel. Both records show highest values during late MIS 3 and MIS 2 (~18 and 30 kyr BP) with several centennial to millennial-scale pulses reaching values of up to ~8% (>150 μm fraction) and counts of up to ~30,000 grains. The most pronounced pulses occur at ~27, 23–25, 21, 19.5–20, and 18 kyr BP. In the earlier part of the records, a number of smaller IRD peaks are present, the most pronounced occurring at ~41.5 and 52.5–54 kyr BP (Figures 4b and 4c).

[28] The relative abundances of $C_{37:4}$ alkenone were compared to IRD estimates in order to constrain their applicability as a paleosalinity proxy. $C_{37:4}$ alkenones are a compound of the alkenone analysis. It has been proposed that these particular alkenones are linked to low-salinity water masses and that a $C_{37:4}$ increase of about 5 to 10% corresponds to a freshening of one practical salinity unit (PSU) [*Rosell-Melé*, 1998; *Rosell-Melé et al.*, 2002]. It is still unclear if indeed salinity has a direct effect on the $C_{37:4}$ biosynthesis or if the observed pattern is due to a metabolic difference of coccolithophorids endemic of cold or coastal water masses [*Schulz et al.*, 2000]. However, even if the production of this alkenone is related to different species of coccoliths, the relative abundances of $C_{37:4}$ may still be used to study the input of fresh-waters [*Bard et al.*, 2000]. $C_{37:4}$ alkenone relative abundances in core MD07-3128 are very low (<5%) during the Holocene and during some intervals of MIS 3 (Figure 4d). Values are substantially higher during the

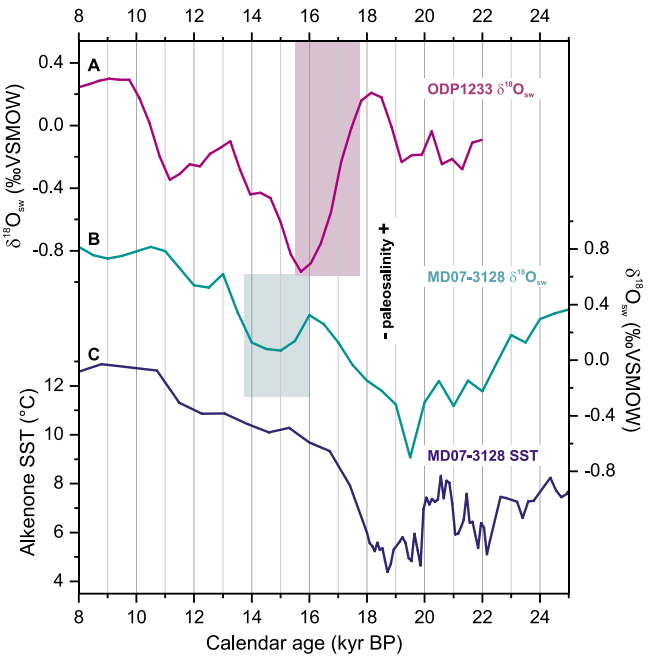

Figure 5. Impacts of Antarctic waters and PIS melting on sea surface salinity between 25 and 8 kyr. (a) $\delta^{18}O_{sw}$ record from ODP Site 1233 (41°S) [*Lamy et al.*, 2004]; vertical bar marks major meltwater pulse. (b) $\delta^{18}O_{sw}$ record from core MD07-3128 (53°S) (this study); vertical bar marks potential meltwater pulse. (c) Alkenone-based SST reconstruction from core MD07-3128 (53°S) (this study).

last glacial in particular during late MIS 3 and MIS 2 with mean relative abundances in the range of 10 to 20%. A number of short-term (centennial to millennial-scale) spikes in $C_{37:4}$ alkenone relative abundance (up to 40%) occur between ~18 and 30 kyr BP. These partly coincide with higher coarse fraction and IRD contents (Figures 4b, 4c, and 4d). In contrast to the IRD proxies that abruptly decrease at ~18 kyr BP, $C_{37:4}$ alkenone relative abundance remains high into the deglaciation until the beginning of the Holocene. Our $\delta^{18}O_{sw}$ reconstruction covering the period from 8 to 25 kyr BP reveals a pronounced ~1‰ decline culminating around 19.5 kyr BP. Thereafter across the deglaciation $\delta^{18}O_{sw}$ stepwise increases reaching values of ~0.8‰ during the early Holocene, i.e., ~0.4‰ heavier than at 25 kyr BP and ~1.5‰ heavier than during the LGM (Figure 5b).

5. Discussion

5.1. Sea Surface Temperatures: Antarctic Timing With Regional Overprint

[29] Despite age uncertainties, alkenone-derived SSTs and planktonic $\delta^{18}O$ in core MD07-3128 generally follow an "Antarctic timing" as also observed in ice cores and marine records further north along the Chilean margin, at ODP Site 1233 [*Lamy et al.*, 2004, 2007; *Kaiser et al.*, 2005] (Figure 3). Although this pattern is particularly evident for the deglacial warming, it also includes the millennial-scale variations during the last glacial. The "Antarctic timing" is consistent with the bipolar seesaw concept of anti-phased temperature changes on the Northern and Southern hemispheres that applies for the last glacial [*EPICA Community Members*, 2006] and extends into Termination 1 [e.g., *Lamy et al.*, 2007]. Recent work further suggests that atmospheric teleconnections play an important role for explaining antiphased temperature signals in both hemispheres [*Denton et al.*, 2010; *Lamy et al.*, 2010; *Lee et al.*, 2011].

[30] The relatively large SST amplitude both over Termination 1 and, on millennial time-scales, during the last glacial suggests an exceptionally strong SST sensitivity at site MD07-3128. The SST changes are even larger than at ODP Site 1233 (Figure 3a) where ~6°C glacial SST cooling has been interpreted in terms of a ~5–6° northward shift of the northern margin of the ACC system in connection with an expansion of the sea ice cover around Antarctica and a northward displacement of the SWW [e.g., *Lamy et al.*, 2004; *Kaiser et al.*, 2005]. Considering that our study area off the Strait of Magellan is presently located ~5° latitude north of the present SAF [*Orsi et al.*, 1995], our study area could have been in the vicinity or even south of the SAF during the coldest times of the last glacial if substantial northward movements of the SO fronts occurred. This interpretation would imply that latitudinal shifts of the SO fronts in the SE-Pacific were much more pronounced than those occurring further west in the central Pacific [*Gersonde et al.*, 2005] (see also 5.2). Strong latitudinal shifts of the SO fronts have also been derived from a dinoflagellate cyst record of ODP Site 1233 [*Verleye and Louwye*, 2010]. The authors interpret a ~7–10° northward shift of the system and even positioned the LGM Polar Front Zone (PFZ) at the latitude of ODP Site 1233. However, these results are inconsistent with the coccolithophore assemblages at the same site [*Saavedra-Pellitero et al.*, 2011], which suggest a more limited northward movement of the assemblages (fronts) of the order of ~5° latitude.

[31] Despite the general "Antarctic timing" of our new southernmost Chilean margin SST record at millennial-time scales and during Termination 1, long-term temperature trends in our record differ from those observed at ODP Site 1233 and in EPICA Antarctic ice core (Figures 3a and 3c). We infer that these diverging long-term trends reflect regional differences in the SST evolution off the Strait of Magellan most likely due to the impact of meltwater and icebergs originating from the southern PIS located close to site MD07-3128, at least during the LGM (see below).

5.2. Dynamics of the PIS

[32] During the last glacial, the icefields in Patagonia expanded to form the larger PIS covering the southern Andes between 36 and 55°S. An updated view of glacial and deglacial changes in the extension of the southern PIS has been recently presented by *Sugden et al.* [2009] based on extensive dating of terrestrial records on the eastern side of the ice sheet. These data suggest five major advances of the southern PIS and/or stagnation phases of the deglacial ice retreat, named Stages A-E (Figure 4a). The oldest Stage A has been tentatively correlated to MIS 4 and is thus beyond the reach of our marine record. During stages B and C (23.1–25.6 kyr BP, and 20.4–21.7 kyr BP) glaciers were at their maximum extent and discharged directly onto outwash plains east of the Andean crest. Particularly Stage B correlates with three pulses of IRD (Figure 4) whereas stage C is only reflected by a relatively minor IRD peak in our record. The same applies to advance D at ~17.7 kyr BP during which glaciers where more restricted and terminated in lakes [*Sugden et al.*, 2009].

[33] This consistency of our IRD changes with the independently dated terrestrial record provides not only confidence in our age model but also suggests that both the Atlantic and the Pacific sides of the southern PIS reacted, within age uncertainties, in phase. Further evidence that the extent changes of the PIS were coherent over large-scales comes from the terrigenous sediment input (Ti and Fe content maxima) at ODP Site 1233 related to northern PIS activity [*Lamy et al.*, 2004; *Kaiser and Lamy*, 2010]. Maxima in glaciogenic sediment input from the northern PIS generally correlate with IRD maxima in our record suggesting coeval millennial-scale variations of the complete PIS during the last glacial. Both ODP Site 1233 and the continental Patagonian records have been compared to dust input changes in Antarctic ice cores [*Sugden et al.*, 2009; *Kaiser and Lamy*, 2010] suggesting a mechanistic link of PIS advances to dust maxima in Antarctica involving the ice sheet derived supply of fine-grained sediment to the Patagonian dust source areas. Our new IRD record is largely consistent with this interpretation and extends the terrestrial record of ice sheet advances back into MIS 3 (Figure 4). Although the comparison to the terrestrial record suggests that our IRD record primarily documents ice sheet advances, we are aware that wind changes were probably likewise important. Strong SWW would reduce the offshore movement of icebergs from the southern PIS. However, it is likely that during glacier advances (primarily cold phases during the glacial) the SWW intensities would have been slightly reduced off southernmost Chile as the core of the SWW moved northward [*Lamy*

et al., 2004, 2007]. Thus, the offshore advection of icebergs would have been facilitated during intervals of southern PIS advances.

[34] Furthermore, the proximal location of our site MD07-3128 to the PIS may also explain the long term SST cooling trend from ~25 kyr to 19 kyr BP (Figure 3a). Our IRD record and the continental evidences [*Sugden et al.*, 2009] suggest that the ice sheet extension was at its maximum during this time interval. It is likely that the supply of meltwater induced a locally enhanced SST cooling close to the ice sheet margin consistent with the fact that no similar long-term cooling is observed at ODP Site 1233 (or any other high resolution SST records from the Chilean margin) nor is it seen in Antarctic ice core records (Figure 3). Furthermore, the ice sheet likely supplied large amounts of meltwater thus reducing sea surface salinities at our site. Reduced paleosalinity at Site MD07-3128 during the glacial are coherent with higher relative abundances of $C_{37:4}$ alkenones (Figure 4d). Higher relative abundances of $C_{37:4}$ alkenones have been related to reduced surface ocean salinities in particular in the Nordic Seas [*Rosell-Melé*, 1998; *Rosell-Melé et al.*, 2002] although other studies suggest that the relationship to paleosalinity is not straightforward [*Sikes and Sicre*, 2002]. Relative abundances of $C_{37:4}$ alkenones appear to be higher during most but not all of the millennial to centennial-scale IRD events (Figure 4) implying a strong link between ice sheet extent and regional paleosalinity, also on shorter scales. Interestingly, the $C_{37:4}$ alkenone relative abundances remain comparatively high during the deglaciation suggesting that relatively fresh surface water conditions persist, perhaps due to a continuous supply of meltwater during ice sheet retreat [*Sugden et al.*, 2009].

[35] Our ice-volume corrected planktonic $\delta^{18}O$ record of *N. pachyderma* (sin.) generally follows the alkenone-derived SST changes during the Termination and the glacial millennial-scale variations (Figure 3) suggesting that paleosalinity changes induced by meltwater supply did not penetrate deep enough into the water column to be recorded by this deep-dwelling foraminifera living just below the thermocline [e.g., *Marchant et al.*, 1998]. However, the long-term baseline trends between both records differ. Particularly, the slight trend toward lighter $\delta^{18}O$ from late MIS 3 to the LGM might be interpreted in terms of a freshening of sub-surface water masses or a shallower depth habitat of *N. pachyderma* (sin.) during the coldest intervals around the LGM.

[36] A freshening of surface waters around the LGM is also indicated by our $\delta^{18}O_{sw}$ reconstruction (Figure 5b). However, this record has be regarded with caution, as we reconstructed $\delta^{18}O_{sw}$ by combining alkenone-based SSTs which are likely affected by shallow meltwater supply (as discussed above) with the $\delta^{18}O_{carb}$ *N. pachyderma* (sin.) living probably mainly below the freshwater layer where the temperature evolution may be slightly different. Nevertheless, there is a quite strong signal in $\delta^{18}O_{sw}$ that may reflect either PIS-derived freshwater supply and/or a general water mass signal derived from salinity changes of subantarctic water masses from the ACC. Furthermore, the PIS meltwater signal during the deglaciation differs significantly from the well pronounced meltwater pulse recorded in the $\delta^{18}O_{sw}$ record at ODP Site 1233 (Figure 5a) [*Lamy et al.*, 2004]. In this record, a major negative shift of ~1.3‰ occurring between ~17.5 and 15.5 kyr BP has been linked to the deglacial melting of the northern PIS (Figure 5a). In the MD07-3128 $\delta^{18}O_{sw}$ record the decrease occurs much earlier and culminates around the LGM which cannot reflect the deglacial melting of southern PIS. However, a small additional decrease centered at ~15 kyr BP may relate to the deglacial melting water consistent with reconstructions of the postglacial paleoenvironmental evolution within the fjords at this latitude [*Kilian et al.*, 2003, 2007].

6. Conclusions

[37] Our SST record from the southernmost Chilean margin (53°S) allows for the first time resolving millennial-scale pattern in the Southeast Pacific at the latitude of the main ACC flow. The timing and structure of these millennial-scale patterns and of Termination 1 is consistent with an "Antarctic timing," as observed in ice cores and SST records further north off Chile as well as in the SW Pacific off New Zealand. However, the SST record off the Strait of Magellan also reveals differences including the long-term cooling from ca. 25 kyr BP toward the LGM, which can be associated to the proximal location of site MD07-3128 to the large glacial PIS.

[38] We provide the first continuous IRD record of the Pacific margin of the PIS. Generally higher contents of IRD during late MIS 3 and the LGM can be interpreted as advances of the ice sheet or reduced westward migration of icebergs due to a northward displacement and/or regional weakening of the Southern Westerlies. Superimposed millennial-scale IRD variations correlate (within age uncertainties) with dust input changes recorded in Antarctic ice cores implying a causal link between ice advances and dust availability, as previously suggested [*Sugden et al.*, 2009]. Furthermore, meltwater input during southern PIS advances is at least partly documented by higher relative abundances of $C_{37:4}$ alkenones. The southern PIS meltwater signal during the last termination probably reveals different amplitudes and timing compared to the record from ODP Site 1233.

[39] Whether the large amplitude SST changes off the Strait of Magellan are a regional feature of the easternmost Pacific sector or whether they extend to other parts of the Pacific SO remains to be shown by additional high resolution paleoceanographic records from this region in the future.

[40] **Acknowledgments.** Funding was provided by the Deutsche Forschungsgemeinschaft (DFG) through grants LA 1273/3-2, LA1273/5-1, and KI-456/9-1. C.L. acknowledges support from the COPAS Center (Project FONDAP 15010007) and the Hanse Wissenschaftskolleg, Delmenhorst (Germany). We thank the captain and crew of IMAGES R/V *Marion Dufresne* cruise MD159/PACHIDERME.

References

Antezana, T. (1999), Hydrographic features of Magellan and Fuegian inland passages and adjacent Subantarctic waters, *Sci. Mar.*, *63*, 23–34.

Arz, H. W., F. Lamy, A. Ganopolski, N. Nowaczyk, and J. Patzold (2007), Dominant Northern Hemisphere climate control over millennial-scale glacial sea-level variability, *Quat. Sci. Rev.*, *26*, 312–321, doi:10.1016/j.quascirev.2006.07.016.

Bard, E., et al. (2000), Hydrological impact of Heinrich events in the subtropical northeast Atlantic, *Science*, *289*, 1321–1324.

Barrows, T. T., S. Juggins, P. De Deckker, E. Calvo, and C. Pelejero (2007a), Long-term sea surface temperature and climate change in the Australian-New Zealand region, *Paleoceanography*, *22*, PA2215, doi:10.1029/2006PA001328.

Barrows, T. T., S. J. Lehman, L. K. Fifield, and P. De Deckker (2007b), Absence of cooling in New Zealand and the adjacent ocean during the

Younger Dryas chronozone, *Science*, *318*, 86–89, doi:10.1126/science.1145873.

Bendle, J., A. Rosell-Mele, and P. Ziveri (2005), Variability of unusual distributions of alkenones in the surface waters of the Nordic seas, *Paleoceanography*, *20*, PA2001, doi:10.1029/2004PA001025.

Bianchi, C., and R. Gersonde (2004), Climate evolution at the last deglaciation: The role of the Southern Ocean, *Earth Planet. Sci. Lett.*, 228, 407–424, doi:10.1016/j.epsl.2004.10.003.

Chaigneau, A., and O. Pizarro (2005), Surface circulation and fronts of the South Pacific Ocean, east of 120°W, *Geophys. Res. Lett.*, *32*, L08605, doi:10.1029/2004GL022070.

Coplen, T. B., C. Kendall, and J. Hopple (1983), Comparison of stable isotopic reference samples, *Nature*, *302*, 236–238, doi:10.1038/302236a0.

DaSilva, J. L., J. B. Anderson, and J. Stravers (1997), Seismic facies changes along a nearly continuous 24 degrees latitudinal transect: The fjords of Chile and the northern Antarctic peninsula, *Mar. Geol.*, *143*, 103–123, doi:10.1016/S0025-3227(97)00092-3.

De Pol-Holz, R., L. Keigwin, J. Southon, D. Hebbeln, and M. Mohtadi (2010), No signature of abyssal carbon in intermediate waters off Chile during deglaciation, *Nat. Geosci.*, *3*, 192–195, doi:10.1038/ngeo745.

Denton, G. H., C. J. Heusser, T. V. Lowell, P. I. Moreno, B. G. Andersen, L. E. Heusser, C. Schluchter, and D. R. Marchant (1999), Interhemispheric linkage of paleoclimate during the last glaciation, *Geogr. Ann., Ser. A*, *81*(2), 107–153, doi:10.1111/j.0435-3676.1999.00055.x.

Denton, G. H., R. F. Anderson, J. R. Toggweiler, R. L. Edwards, J. M. Schaefer, and A. E. Putnam (2010), The Last Glacial Termination, *Science*, *328*, 1652–1656, doi:10.1126/science.1184119.

EPICA Community Members (2006), One-to-one coupling of glacial climate variability in Greenland and Antarctica, *Nature*, *444*, 195–198, doi:10.1038/nature05301.

Fairbanks, R. G. (1989), A 17,000-year glacio-eustatic sea-level record - Influence of glacial melting rates on the Younger Dryas event and deep-ocean circulation, *Nature*, *342*, 637–642, doi:10.1038/342637a0.

Fischer, H., et al. (2007), Erratum to "Reconstruction of millennial changes in dust emission, transport and regional sea ice coverage using the deep EPICA ice cores from the Atlantic and Indian Ocean sector of Antarctica" [Earth Planet. Sci. Lett. 260 (2007) 340–354], *Earth Planet. Sci. Lett.*, *262*, 635–636, doi:10.1016/j.epsl.2007.08.016.

Gersonde, R., X. Crosta, A. Abelmann, and L. Armand (2005), Sea-surface temperature and sea ice distribution of the Southern Ocean at the EPILOG Last Glacial Maximum - a circum-Antarctic view based on siliceous microfossil records, *Quat. Sci. Rev.*, *24*, 869–896, doi:10.1016/j.quascirev.2004.07.015.

Glasser, N., and K. Jansson (2008), The glacial map of southern South America, *J. Maps*, 2008, 175–196, doi:10.4113/jom.2008.1020.

Hollin, J. T., and D. H. Schilling (1981), Late Wisconsin-Weichselian mountain glaciers and small ice caps, in *The Last Great Ice Sheets*, edited by G. H. Denton and T. J. Hughes, pp. 179–220, Wiley, New York.

Ingram, B. L., and J. R. Southon (1996), Reservoir ages in eastern Pacific coastal and estuarine waters, *Radiocarbon*, *38*, 573–582.

Jouzel, J., et al. (2007), Orbital and millennial Antarctic climate variability over the past 800,000 years, *Science*, *317*, 793–796, doi:10.1126/science.1141038.

Kaiser, J., and F. Lamy (2010), Links between Patagonian Ice Sheet fluctuations and Antarctic dust variability during the last glacial period (MIS 4–2), *Quat. Sci. Rev.*, *29*, 1464–1471, doi:10.1016/j.quascirev.2010.03.005.

Kaiser, J., F. Lamy, and D. Hebbeln (2005), A 70-kyr sea surface temperature record off southern Chile (ODP Site 1233), *Paleoceanography*, *20*, PA4009, doi:10.1029/2005PA001146.

Kaiser, J., E. Schefuss, F. Lamy, M. Mohtadi, and D. Hebbeln (2008), Glacial to Holocene changes in sea surface temperature and coastal vegetation in north central Chile: High versus low latitude forcing, *Quat. Sci. Rev.*, *27*, 2064–2075, doi:10.1016/j.quascirev.2008.08.025.

Kaplan, M. R., C. J. Fogwill, D. E. Sugden, N. Hulton, P. W. Kubik, and S. Freeman (2008), Southern Patagonian glacial chronology for the Last Glacial period and implications for Southern Ocean climate, *Quat. Sci. Rev.*, *27*, 284–294, doi:10.1016/j.quascirev.2007.09.013.

Kaplan, M. R., J. M. Schaefer, G. H. Denton, D. J. A. Barrell, T. J. H. Chinn, A. E. Putnam, B. G. Andersen, R. C. Finkel, R. Schwartz, and A. M. Doughty (2010), Glacier retreat in New Zealand during the Younger Dryas stadial, *Nature*, *467*, 194–197, doi:10.1038/nature09313.

Kilian, R., M. Hohner, H. Biester, H. J. Wallrabe-Adams, and C. R. Stern (2003), Holocene peat and lake sediment tephra record from the southernmost Chilean Andes (53–55°S), *Rev. Geol. Chile*, *30*(1), 23–37.

Kilian, R., O. Baeza, T. Steinke, M. Arevalo, C. Rios, and C. Schneider (2007), Late Pleistocene to Holocene marine transgression and thermohaline control on sediment transport in the western Magellanes fjord system of Chile (53°S), *Quat. Int.*, *161*, 90–107, doi:10.1016/j.quaint.2006.10.043.

Laj, C., C. Kissel, A. Mazaud, J. E. T. Channell, and J. Beer (2000), North Atlantic palaeointensity stack since 75 ka (NAPIS-75) and the duration of the Laschamp event, *Philos. Trans. R. Soc. A*, *358*(1768), 1009–1025.

Laj, C., C. Kissel, R. Leonhardt, M. Winklofer, A. Ferk, K. Fabian, and U. Ninemann (2009), Towards a global view of the laschamp excursion, *Geophy. Res. Abstr.*, *11* EGU2009-2737-1.

Lamy, F., J. Kaiser, U. Ninnemann, D. Hebbeln, H. Arz, and J. Stoner (2004), Antarctic timing of surface water changes off Chile and Patagonian Ice Sheet response, *Science*, *304*, 1959–1962, doi:10.1126/science.1097863.

Lamy, F., J. Kaiser, H. W. Arz, D. Hebbeln, U. Ninnemann, O. Timm, A. Timmermann, and J. R. Toggweiler (2007), Modulation of the bipolar seesaw in the southeast pacific during Termination 1, *Earth Planet. Sci. Lett.*, *259*, 400–413, doi:10.1016/j.epsl.2007.04.040.

Lamy, F., R. Kilian, H. W. Arz, J. P. Francois, J. Kaiser, M. Prange, and T. Steinke (2010), Holocene changes in the position and intensity of the southern westerly wind belt, *Nat. Geosci.*, *3*, 695–699, doi:10.1038/ngeo959.

Lee, S. Y., J. C. H. Chiang, K. Matsumoto, and K. S. Tokos (2011), Southern Ocean wind response to North Atlantic cooling and the rise in atmospheric CO_2: Modeling perspective and paleoceanographic implications, *Paleoceanography*, *26*, PA1214, doi:10.1029/2010PA002004.

Lemieux-Dudon, B., E. Blayo, J. R. Petit, C. Waelbroeck, A. Svensson, C. Ritz, J. M. Barnola, B. M. Narcisi, and F. Parrenin (2010), Consistent dating for Antarctic and Greenland ice cores, *Quat. Sci. Rev.*, *29*, 8–20, doi:10.1016/j.quascirev.2009.11.010.

Lowell, T. V., C. J. Heusser, B. G. Andersen, P. I. Moreno, A. Hauser, L. E. Heusser, C. Schlüchter, D. R. Marchant, and G. H. Denton (1995), Interhemispheric correlation of Late Pleistocene glacial events, *Science*, *269*, 1541–1549, doi:10.1126/science.269.5230.1541.

Marchant, M., D. Hebbeln, and G. Wefer (1998), Seasonal flux patterns of planktic foraminifera in the Peru-Chile Current, *Deep Sea Res., Part I*, *45*, 1161–1185, doi:10.1016/S0967-0637(98)00009-0.

MARGO Project Members (2009), Constraints on the magnitude and patterns of ocean cooling at the Last Glacial Maximum, *Nat. Geosci.*, *2*, 127–132.

Mashiotta, T. A., D. W. Lea, and H. J. Spero (1999), Glacial-interglacial changes in Subantarctic sea surface temperature and delta O-18-water using foraminiferal Mg, *Earth Planet. Sci. Lett.*, *170*, 417–432, doi:10.1016/S0012-821X(99)00116-8.

McClymont, E. L., A. Rosell-Mele, G. H. Haug, and J. M. Lloyd (2008), Expansion of subarctic water masses in the North Atlantic and Pacific oceans and implications for mid-Pleistocene ice sheet growth, *Paleoceanography*, *23*, PA4214, doi:10.1029/2008PA001622.

McCulloch, R. D., M. J. Bentley, R. S. Purves, N. R. J. Hulton, D. E. Sugden, and C. M. Clapperton (2000), Climatic inferences from glacial and palaeoecological evidence at the last glacial termination, southern South America, *J. Quat. Sci.*, *15*, 409–417, doi:10.1002/1099-1417(200005)15:4<409::AID-JQS539>3.0.CO;2-#.

Mohtadi, M., P. Rossel, C. B. Lange, S. Pantoja, P. Boning, D. J. Repeta, M. Grunwald, F. Lamy, D. Hebbeln, and H. J. Brumsack (2008), Deglacial pattern of circulation and marine productivity in the upwelling region off central-south Chile, *Earth Planet. Sci. Lett.*, *272*, 221–230, doi:10.1016/j.epsl.2008.04.043.

Moreno, P. I., G. L. Jacobson, T. V. Lowell, and G. H. Denton (2001), Interhemispheric climate links revealed by a late-glacial cooling episode in southern Chile, *Nature*, *409*, 804–808, doi:10.1038/35057252.

Moreno, P. I., M. R. Kaplan, J. P. Francois, R. Villa-Martinez, C. M. Moy, C. R. Stern, and P. W. Kubik (2009), Renewed glacial activity during the Antarctic cold reversal and persistence of cold conditions until 11.5 ka in southwestern Patagonia, *Geology*, *37*, 375–378, doi:10.1130/G25399A.1.

Müller, P. J., G. Kirst, G. Ruhland, I. von Storch, and A. Rosell-Mele (1998), Calibration of the alkenone paleotemperature index UK′37 based on core-tops from the eastern South Atlantic and the global ocean (60°N–60°S), *Geochim. Cosmochim. Acta*, *62*, 1757–1772, doi:10.1016/S0016-7037(98)00097-0.

Orsi, A. H., T. Whitworth, and W. D. Nowlin (1995), On the meridional extent and fronts of the Antarctic Circumpolar Current, *Deep Sea Res., Part I*, *42*, 641–673, doi:10.1016/0967-0637(95)00021-W.

Pahnke, K., R. Zahn, H. Elderfield, and M. Schulz (2003), 340,000-year centennial-scale marine record of Southern Hemisphere climatic oscillation, *Science*, *301*, 948–952, doi:10.1126/science.1084451.

Pickard, G. L. (1971), Some physical oceanographic features of inlets of Chile, *J. Fish. Res. Board Can.*, *28*(8), 1077–1106, doi:10.1139/f71-163.

Prahl, F. G., and S. G. Wakeham (1987), Calibration of unsaturation patterns in long-chain ketone compositions for paleotemperature assessment, *Nature*, *330*, 367–369, doi:10.1038/330367a0.

Prahl, F. G., L. A. Muehhausen, and D. L. Zahnle (1988), Further evaluation of long-chain alkenones as indicators of paleoceanographic conditions, *Geochim. Cosmochim. Acta*, *52*, 2303–2310, doi:10.1016/0016-7037(88)90132-9.

Reimer, P. J., et al. (2009), IntCal09 and Marine09 radiocarbon age calibration curves, 0–50,000 years cal BP, *Radiocarbon*, *51*, 1111–1150.

Romero, O., J. H. Kim, and D. Hebbeln (2006), Paleoproductivity evolution off central Chile from the Last Glacial Maximum to the Early Holocene, *Quat. Res.*, *65*, 519–525, doi:10.1016/j.yqres.2005.07.003.

Rosell-Melé, A. (1998), Interhemispheric appraisal of the value of alkenone indices as temperature and salinity proxies in high-latitude locations, *Paleoceanography*, *13*, 694–703, doi:10.1029/98PA02355.

Rosell-Melé, A., E. Jansen, and M. Weinelt (2002), Appraisal of a molecular approach to infer variations in surface ocean freshwater inputs into the North Atlantic during the last glacial, *Global Planet. Change*, *34*, 143–152, doi:10.1016/S0921-8181(02)00111-X.

Rostek, F., G. Ruhland, F. C. Bassinot, P. J. Muller, L. D. Labeyrie, Y. Lancelot, and E. Bard (1993), Reconstructing sea-surface temperature and salinity using δ^{18}O and alkenone records, *Nature*, *364*, 319–321, doi:10.1038/364319a0.

Saavedra-Pellitero, M., J. A. Flores, F. Lamy, F. J. Sierro, and A. Cortina (2011), Coccolithophore estimates of paleotemperature and paleoproductivity changes in the southeast Pacific over the past ~27 kyr, *Paleoceanography*, *26*, PA1201, doi:10.1029/2009PA001824.

Schulz, H.-M., A. Schöner, and K.-C. Emeis (2000), Long-chain alkenone patterns in the Baltic Sea -an ocean-freshwater transition, *Geochim. Cosmochim. Acta*, *64*, 469–477, doi:10.1016/S0016-7037(99)00332-4.

Shackleton, N. J. (1974), Attainment of isotopic equilibrium between ocean water and the benthic foraminifera genus uvigerina: Isotopic changes in the ocean during the last glacial, in *Les Méthodes Quantitatives d'Étude des Variations du Climat au Cours du Pléistocène*, vol. 219, edited by L. Labeyrie, pp. 203–209, CNRS, Paris.

Shaffer, G., S. Salinas, O. Pizarro, A. Vega, and S. Hormazabal (1995), Currents in the deep ocean off Chile (30°S), *Deep Sea Res., Part I*, 42, 425–436, doi:10.1016/0967-0637(95)99823-6.

Sievers, H. A., and N. Silva (2008), Water masses and circulation in austral Chilean channels and fjords, in *Progress in the Oceanographic Knowledge of Chilean Interior Waters, From Puerto Montt to Cape Horn*, edited by N. Silva and S. Palma, pp. 53–58, Com. Oceanogr. Nac., Pontif. Univ. Católica de Valparaíso, Santiago.

Sikes, E. L., and M. A. Sicre (2002), Relationship of the tetra-unsaturated C-37 alkenone to salinity and temperature: Implications for paleoproxy applications, *Geochem. Geophys. Geosyst.*, *3*(11), 1063, doi:10.1029/2002GC000345.

Sikes, E. L., J. K. Volkman, L. G. Robertson, and J.-J. Pichon (1997), Alkenones and alkenes in surface waters and sediments of the Southern Ocean: Implications for paleotemperature estimation in polar regions, *Geochim. Cosmochim. Acta*, *61*, 1495–1505, doi:10.1016/S0016-7037(97)00017-3.

Silva, N., and C. Calvete (2002), Physical and chemical oceanographic features of southern Chilean inlets between Penas Gulf and Magellan Strait (CIMAR-FIORDO 2 CRUISE), *Cienc. Tecnol. Mar*, *25*(1), 23–28.

Stocker, T. F., and S. J. Johnsen (2003), A minimum thermodynamic model for the bipolar seesaw, *Paleoceanography*, *18*(4), 1087, doi:10.1029/2003PA000920.

Strub, P. T., J. M. Mesias, V. Montecino, J. Ruttlant, and S. Salinas (1998), Coastal ocean circulation off Western South America, in *The Sea*, vol. 11, *The Global Coastal Ocean: Regional Studies and Syntheses*, edited by A. R. Robinson and K. H. Brink, pp. 273–315, Wiley, New York.

Sugden, D. E., R. D. McCulloch, A. J. M. Bory, and A. S. Hein (2009), Influence of Patagonian glaciers on Antarctic dust deposition during the last glacial period, *Nat. Geosci.*, *2*, 281–285, doi:10.1038/ngeo474.

Verleye, T., and S. Louwye (2010), Late Quaternary environmental changes and latitudinal shifts of the Antarctic Circumpolar Current as recorded by dinoflagellate cyst from offshore Chile (41°S), *Quat. Sci. Rev.*, *29*, 1025–1039, doi:10.1016/j.quascirev.2010.01.009.

C. Aracena, Graduate Programme in Oceanography, University of Concepción, PO Box 160-C, Concepción, Chile.

H. Arz and J. Kaiser, Leibniz Institute for Baltic Sea Research Warnemünde, Seestraße 15, D-18119 Rostock-Warnemünde, Germany.

O. Baeza Urrea and R. Kilian, Lehrstuhl für Geologie, Universität Trier, Behringstraße, D-54286 Trier, Germany.

M. Caniupán, F. Lamy, G. Mollenhauer, and R. Tiedemann, Alfred Wegener Institute for Polar and Marine Research, Am Handelshafen 12, D-27570 Bremerhaven, Germany. (frank.lamy@awi.de)

D. Hebbeln, MARUM–Center for Marine Environmental Sciences, University of Bremen, Leobener Strasse, D-28359 Bremen, Germany.

C. Kissel and C. Laj, Laboratoire des Sciences du Climat et de l'Environnement, Institut Pierre Simon Laplace, Bâtiment 12, Av. de la Terrasse, F-91198 Gif-sur-Yvette CEDEX, France.

C. B. Lange, Department of Oceanography and Center for Oceanographic Research in the Eastern South Pacific, University of Concepción, PO Box 160-C, Concepción, Chile.